BioRisk 18: 93–104 (2022)
doi: 10.3897/biorisk.18.80607
https://biorisk.pensoft.net

RESEARCH ARTICLE

A peer-reviewed open-access journal
BioRisk

Potential risk resulting from the influence of static magnetic field upon living organisms. Numerically simulated effects of the static magnetic field upon porphine

Wojciech Ciesielski[1], Tomasz Girek[1], Zdzisław Oszczęda[2], Jacek A. Soroka[3], Piotr Tomasik[2]

1 *Institute of Chemistry, Jan Długosz University, 42 201 Częstochowa, Poland* **2** *Nantes Nanotechnological Systems, 59 700 Bolesławiec, Poland* **3** *Scientific Society of Szczecin, 71-481 Szczecin, Poland*

Corresponding author: Wojciech Ciesielski (w.ciesielski@interia.pl)

Academic editor: Josef Settele | Received 16 January 2022 | Accepted 9 May 2022 | Published 30 June 2022

Citation: Ciesielski W, Girek T, Oszczeda Z, Soroka JA, Tomasik P (2022) Potential risk resulting from the influence of static magnetic field upon living organisms. Numerically simulated effects of the static magnetic field upon porphine. BioRisk 18: 93–104. https://doi.org/10.3897/biorisk.18.80607

Abstract

Background: Recognizing effects of static magnetic field (SMF) of varying flux density on flora and fauna is attempted. For this purpose the influence of SMF upon the porphine molecule is studied.

Methods: Computations of the effect of static magnetic field (SMF) of 0.0, 0.1, 1, 10 and 100 AFU (1 AFU > 1000 T) flux density were performed in silico for SMF changes distribution of the electron density in that molecule. HyperChem 8.0 software was used together with the AM1 method for optimization of the conformation of the molecule of porphine. The computations of polarizability, charge distribution, potential and dipole moment for molecules placed in SMF were performed for molecule situated subsequently in the x-y, y-z and x-z planes of the Cartesian system. The computations involved the DFT 3-21G method.

Results: Static magnetic field (SMF) decreased stability of the porphine molecule. This effect depended on the situating the molecule in respect to the direction of SMF of the Cartesian system. An increase in the value of heat of formation was accompanied by an increase in dipole moment.

Conclusions: Observed effects resulted from deformations of the molecule which involved pyrrole rings holding the hydrogen atoms at the ring nitrogen atoms and the length of the C–H and N–H bonds. In a consequence that macrocyclic ring lost its planarity.

Keywords

dipole moment, heat of formation, structure deformation

Introduction

Although porphine itself (Fig. 1) does not occur in nature, numerous porphine derivatives play an essential role in functioning in living organisms of flora and fauna.

Porphine is a macrocyclic compound of an aromatic character. It is formed of four pyrrole rings bound with four methine (-CH=) bridges. The macrocyclic ring is planar and only the N–H bonds are bent in opposite (*trans*) directions (Caughey and Ibers 1977; Kadish et al. 2000; Ortiz de Montellano 2008). Involving numerous biosynthetic ways (Elder 1994; Aylward and Bofinger 2005), many porphine derivatives are naturally formed from protoporhyrin IX, it being a precursor of several biologically important compounds. A biological activity of porphine derivatives is achieved when metal ions are coordinated within the macrocyclic ring (Caughey and Ibers 1977; Kadish et al. 2000; Ortiz de Montellano 2008). This course of study was developed as a consequence of considerable environmental pollution with magnetic fields generated by modern technologies and technical solutions in several areas of human everyday life (Hamza et al. 2002; Rankovic and Radulovic 2009; Committee to Assess the Current Status and Future Direction of High Magnetic Field Science in the United States 2013; Magnet Science and Technology 2021; Magnetism in real life 2021). This paper follows a series of three recent papers of ours in which the effect of static magnetic field (SMF) upon small inorganic molecules (Ciesielski et al. 2021), lower alkanols (Ciesielski et al. 2022a) and monosaccharides (Ciesielski et al. 2022b) was recognized. In order to recognize the effect of SMF upon biologically important

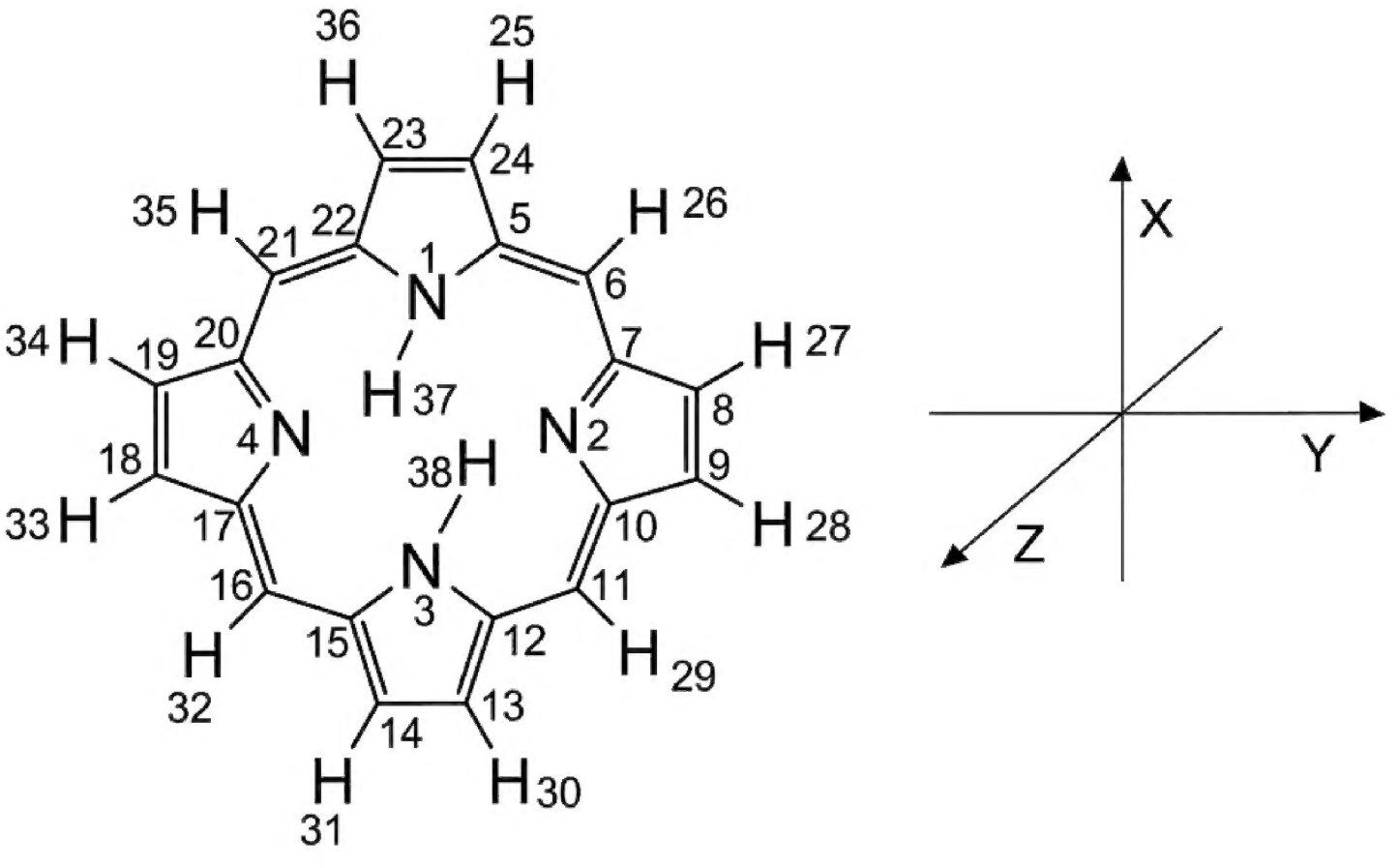

Figure 1. Structure of the porphine molecule with the system of numbering of the atoms followed throughout the discussion and situating axes of the Cartesian system.

metalloporphyrines, in the present study we focused on the effect of SMF upon their free ligand, i.e. porphine itself.

As in our former papers (Ciesielski et al. 2021; Ciesielski et al. 2022a, b) the effect of SMF of flux density varying from 0 to 100 AFU was simulated with advanced numerical computations involving the in silico approach.

Numerical computations

DFT Molecular structures were drawn using the Fujitsu Scigress 2.0 software (Marchand et al. 2014). Their principal symmetry axes were oriented along the x-, y and z-axes of the Cartesian system. The magnetic field was fixed in the same direction with the south pole from the left side. Z axis is directed perpendicularly to the porphine plane, the x and y axes are in the plane of the system, each of them along two nitrogen atoms. In the case of full mesomerism, because of the quaternary symmetry of z axis, the last two axes were undistinguished. When the nitrogen atoms differ from one another, the x axis crossed two nitrogen atoms substituted by hydrogen atoms and y axis crossed remained two unsubstituted nitrogen atoms. Thus, both x and y axes were distinguishable.

Subsequently, utilizing Gaussian 0.9 software equipped with the 6-31G** basis (Frisch et al. 2016), the molecules were optimized and all values of bond length, dipole moment, heath of formation, bond energy, HOMO/LUMO energy level for single molecules as well as HOMO/LUMO energy level and total energy for systems built of three molecules, were computed.

In the consecutive step, the influence of the static magnetic field (SMF) upon optimized molecules was computed with Amsterdam Modelling Suite software (Farberovich and Mazalova 2016; Charistos and Muñoz-Castro 2019) and the NR_LDOTB (non-relativistic orbital momentum L-dot-B) method (Glendening et al. 1987; Carpenter and Weinhold 1988). Following that step, using Gaussian 0.9 software equipped with the DFT with functional B3LYP 6-31G** basis (Frisch et al. 2016) the values of bond length, dipole moment, heath of formation equal to the energy of dissociation, bond energy HOMO/LUMO energy level for single molecules, were again computed using the single-point energy option key word.

Visualization of the HOMO/LUMO orbitals and changes of the electron density for particular molecules and their three molecule systems was performed involving the HyperChem 8.0 software (Froimowitz 1993; Mazurkiewicz and Tomasik 2013).

Results and discussion

Generally, SMF decreased stability of the poprhine molecule (Table 1). Heat of formation increased with an increase in applied flux density. This effect depended on the positioning of the molecule in respect to the direction of SMF defined in terms

of the Cartesian system. The response of the molecule in the x-y, y-z and x-z planes did not parallel one another. An increase in the value of heat of formation was accompanied by an increase in dipole moment. Again, these changes did not parallel one another.

Thus, SMF destabilized porphine, increasing interatomic distances and separating their charges.

Heat of formation and dipole moments regularly, although to a different extent, increased with an increase in the applied SMF flux density. This effect was common for porphine molecule, regardless whether it was located in either the x-y, y-z or x-z plane. However, in terms of dipole moment, the strongest reaction to an increase in flux density was noted for the molecule situated in the x-y plane.

These total effects resulted from the distribution of the charge density at particular atoms, bond lengths, the deformation of the molecules and changes of their initial position in selected plane of the Cartesian system. Table 2 shows that, usually, charge density at particular atoms changed irregularly against an increase in the SMF flux density. The irregularity in associated bond lengths is shown in Table 3.

Table 2 revealed that the highest number of irregular changes of the charge distribution against changes of flux density was met in the molecule situated in the x-y and y-z planes, whereas the number of such irregularities in the x-z plane was minute. It should also be noted that several cases of a lack of sensitivity of the charge density to an increase in the flux density were observed when the molecule was oriented in the x-z plane.

The highest number of irregular changes of the bond lengths against an increase in flux density was observed for the molecule situated in the x-y plane.

Fig. 2 presents deformation of this molecule situated in the x-y, y-z and x-z planes of the Cartesian system.

One might see that, first of all, regardless of the positioning of the molecule in the Cartesian system, the deformation involved pyrrole rings holding the hydrogen atoms at the ring nitrogen atoms and the length of the C–H and N–H bonds. The magnitudes of the deformation are well illustrated by a variation of the charge density at particular atoms (Table 2) and corresponding bond lengths (Table 3). Particularly, but not solely, structures of the molecule situated in the y-z plane show that the macrocyclic ring lost its planarity. Porphine treated with external electric field behaved similarly (Mazurkiewicz and Tomasik 2013).

Table 1. Heat of formation [kJ.mol^{-1}] and dipole moment [D] of the porphine molecule depending on its positioning in the Cartesian system and applied SMF flux density [AFU].

Orientation along the axes of the Cartesian System	Heat of formation [kJ·mol^{-1}] at SMF flux density [AFU]					Dipole moment [D] at SMF flux density [AFU]				
	0	**0.1**	**1.0**	**10**	**100**	**0**	**0.1**	**1.0**	**10**	**100**
x-y	-792	-782	-758	-731	-704	2.01	2.12	2.48	2.88	3.09
y-z	-792	-789	-765	-742	-711	2.01	2.03	2.11	2.16	2.63
x-z	-792	-781	-763	-715	-697	2.01	2.06	2.34	2.74	2.89

Table 2. Charge density [a.u] at particular atoms of the porphine molecule depending on SMF flux density [AFU] positioning in the Cartesian system.

Atom	SMF along indicated Cartesian axis	Tendency*	Charge density [a.u] at SMF flux density [AFU]				
			0	**0.1**	**1.0**	**10**	**100**
N1	X	**RH**	-1.119	-1.045	-0.987	-0.985	-0.937
	Z	**RH**		-1.025	-1.017	-1.012	-0.934
	Y	**IH**		-1.004	-0.789	-0.940	-0.545
N2	X	**IL**	-0.817	-0.807	-0.795	-0.813	-0.855
	Z	**RH**		-0.783	-0.779	-0.772	-0.756
	Y	**V**		-0.750	-0.684	-0.425	-0.725
N3	X	**IH**	-1.089	-1.025	-0.993	-0.948	-0.985
	Z	**IL**		-0.988	-0.986	-0.991	-0.995
	Y	**IH**		-1.035	-0.938	-0.978	-0.789
N4	X	**RH**	-0.817	-0.816	-0.795	-0.762	-0.754
	Z	**IH**		-0.785	-0.779	-0.785	-0.765
	Y	**V**		-0.662	-0.759	-0.503	-0.454
C5	X	**IH**	0.492	0.454	0.359	0.447	0.572
	Z	**IL**		0.450	0.457	0.431	0.391
	Y	**RL**		0.474	0.282	0.152	0.070
C6	X	**IH**	-0.355	-0.351	-0.312	-0.317	-0.283
	Z	**NC**		-0.354	-0.362	-0.350	-0.348
	Y	**IH**		-0.370	-0.148	-0.121	-0.094
C7	X	**IL**	0.393	0.362	0.310	0.354	0.285
	Z	**NC**		0.384	0.380	0.385	0.383
	Y	**RL**		0.332	0.269	0.163	-0.283
C8	X	**IH**	-0.283	-0.251	-0.267	-0.244	-0.197
	Z	**NC**		-0.274	-0.272	-0.278	-0.273
	Y	**IH**		-0.219	-0.077	-0.007	-0.163
C9	X	**RL**	-0.213	-0.214	-0.233	-0.249	-0.257
	Z	**NC**		-0.226	-0.223	-0.221	-0.222
	Y	**V**		-0.150	-0.150	-0.232	-0.059
C10	X	**RH**	0.282	0.285	0.286	0.305	0.353
	Z	**IL**		0.281	0.278	0.254	0.262
	Y	**IL**		0.220	0.105	0.185	-0.088
C11	X	**V**	-0.253	-0.273	-0.227	-0.301	-0.298
	Z	**V**		-0.296	-0.291	-0.273	-0.268
	Y	**V**		-0.116	-0.202	-0.235	-0.001
C12	X	**V**	0.434	0.418	0.330	0.425	0.476
	Z	**V**		0.389	0.392	0.371	0.409
	Y	**IL**		0.339	0.255	0.260	0.226
C13	X	**V**	-0.292	-0.305	0.018	0.338	0.470
	Z	**V**		-0.266	-0.269	-0.241	-0.272
	Y	**V**		-0.353	-0.207	-0.152	0.356
C14	X	**IH**	-0.292	-0.249	-0.309	0.037	0.023
	Z	**V**		-0.269	-0.269	-0.282	-0.268
	Y	**V**		-0.291	-0.372	-0.184	-0.348
C15	X	**V**	0.434	0.354	0.419	0.247	0.209
	Z	**IL**		0.397	0.392	0.418	0.385
	Y	**RL**		0.410	0.389	0.290	0.094
C16	X	**IH**	-0.253	-0.221	-0.322	-0.139	-0.189
	Z	**IL**		-0.295	-0.291	-0.303	-0.311
	Y	**V**		-0.311	-0.073	-0.103	-0.089

Atom	SMF along indicated Cartesian axis	Tendency*	Charge density [a.u] at SMF flux density [AFU]				
			0	0.1	1.0	10	100
C17	X	**V**	0.282	0.281	0.309	0.243	0.256
	Z	**RL**		0.278	0.278	0.277	0.257
	Y	**RL**		0.252	0.230	0.148	-0.051
C18	X	**NC**	-0.213	-0.201	-0.233	-0.206	-0.207
	Z	**NC**		-0.224	-0.223	-0.224	-0.224
	Y	**IH**		-0.197	-0.127	-0.095	-0.067
C19	X	**V**	-0.283	-0.272	-0.249	-0.274	-0.272
	Z	**V**		-0.272	-0.272	-0.265	-0.274
	Y	**IH**		-0.163	-0.183	-0.189	-0.124
C20	X	**RL**	0.393	0.356	0.348	0.288	0.275
	Z	**NC**		0.388	0.379	0.393	0.400
	Y	**V**		0.235	0.243	0.263	0.113
C21	X	**V**	-0.355	-0.352	-0.360	-0.218	-0.095
	Z	**NC**		-0.363	-0.359	-0.349	-0.375
	Y	**IH**		-0.232	-0.238	-0.146	-0.123
C22	X	**RL**	0.492	0.428	0.419	0.292	0.169
	Z	**RL**		0.470	0.456	0.456	0.442
	Y	**IL**		0.367	0.338	0.183	0.276
C23	X	**V**	-0.230	-0.210	-0.052	-0.175	-0.152
	Z	**NC**		-0.241	-0.241	-0.242	-0.240
	Y	**IH**		-0.133	-0.175	-0.129	-0.019
C24	X	**V**	-0.230	-0.160	-0.223	0.026	-0.032
	Z	**NC**		-0.242	-0.241	-0.234	-0.232
	Y	**V**		-0.288	-0.112	-0.140	-0.021
H25	X	**V**	0.267	0.209	0.290	0.258	-0.071
	Z	**NC**		0.265	0.264	0.273	0.270
	Y	**V**		0.269	0.126	0.077	0.127
H26	X	**V**	0.230	0.217	0.234	0.260	0.237
	Z	**NC**		0.239	0.235	0.232	0.233
	Y	**IL**		0.214	0.069	0.077	0.103
H27	X	**V**	0.240	0.235	0.234	0.270	0.268
	Z	**IL**		0.239	0.241	0.235	0.232
	Y	**V**		0.179	0.175	0.179	0.151
H28	X	**NC**	0.250	0.247	0.245	0.250	0.247
	Z	**NC**		0.246	0.246	0.249	0.251
	Y	**IL**		0.192	0.168	0.179	0.166
H29	X	**NC**	0.254	0.248	0.259	0.260	0.258
	Z	**NC**		0.255	0.252	0.251	0.250
	Y	**IL**		0.170	0.197	0.151	0.075
H30	X	**V**	0.237	0.247	0.018	0.234	0.188
	Z	**NC**		0.245	0.244	0.238	0.243
	Y	**V**		0.080	0.220	0.180	0.027
H31	X	**V**	0.237	0.059	0.256	0.060	0.071
	Z	**NC**		0.243	0.244	0.237	0.238
	Y	**IL**		0.245	0.122	0.120	0.061
H32	X	**IL**	0.254	0.242	0.253	0.218	0.206
	Z	**NC**		0.253	0.252	0.256	0.258
	Y	**IL**		0.261	0.149	0.114	0.099
H33	X	**V**	0.250	0.237	0.250	0.233	0.189
	Z	**NC**		0.246	0.246	0.242	0.244
	Y	**RL**		0.216	0.174	0.167	0.132

Atom	SMF along indicated Cartesian axis	Tendency*	Charge density [a.u] at SMF flux density [AFU]				
			0	0.1	1.0	10	100
H34	X	**V**	0.240	0.233	0.252	0.238	0.218
	Z	**NC**		0.241	0.241	0.244	0.247
	Y	**V**		0.159	0.169	0.288	0.179
H35	X	**V**	0.230	0.232	0.248	0.233	0.244
	Z	**NC**		0.236	0.236	0.227	0.234
	Y	**IL**		0.126	0.139	0.099	0.055
H36	X	**V**	0.267	0.257	0.054	0.339	0.244
	Z	**NC**		0.264	0.264	0.256	0.253
	Y	**V**		0.177	0.207	0.165	0.035
H37	X	**NC**	0.474	0.474	0.479	0.481	0.441
	Z	**IL**		0.452	0.446	0.447	0.434
	Y	**V**		0.585	0.402	0.091	0.378
H38	X	**RH**	0.461	0.485	0.489	0.492	0.530
	Z	**RL**		0.454	0.447	0.445	0.442
	Y	**V**		0.484	0.508	0.048	0.594

*Abbreviations used here and in next Tables: RHregularly increasing, IH - irregularly increasing, RL- regularly decreasing, IL - irregularly decreasing, V - lack of any regular tendency, NC - nearly constant.

Table 3. Bond lengths [Å] between particular atoms of the porphine molecule depending on SMF flux density [AFU] positioning in the Cartesian system. See Table 2 for notation.

Bond	SMF along indicated Cartesian axis	Tendency*	Bond length [Å] at flux density [AFU]				
			0	0.1	1.0	10	100
N1-C5	X	**IL**	1.326	1.352	1.409	1.373	1.387
	Z	**IH**		1.385	1.402	1.390	1.463
	Y	**IH**		1.358	1.451	1.640	1.502
N1-C22	X	**RH**	1.340	1.354	1.381	1.434	1.438
	Z	**V**		1.407	1.402	1.405	1.425
	Y	**IH**		1.417	1.430	1.552	1.432
N1-H37	X	**NC**	1.010	1.112	1.040	1.055	1.108
	Z	**V**		0.990	0.990	0.975	0.985
	Y	**IH**		1.052	1.480	1.732	1.727
N2-C7	X	**V**	1.325	1.357	1.392	1.357	1.345
	Z	**V**		1.432	1.337	1.321	1.320
	Y	**IH**		1.422	1.349	1.448	1.552
N2-C10	X	**V**	1.401	1.410	1.374	1.411	1.379
	Z	**V**		1.432	1.425	1.433	1.431
	Y	**IH**		1.458	1.593	1.579	1.676
N3-C12	X	**IH**	1.328	1.358	1.367	1.389	1.370
	Z	**V**		1.384	1.391	1.375	1.368
	Y	**V**		1.303	1.416	1.484	1.226
N3-C15	X	**RH**	1.328	1.347	1.389	1.404	1.435
	Z	**V**		1.394	1.391	1.392	1.395
	Y	**V**		1.359	1.270	1.358	1.277
N3-H38	X	**NC**	1.010	1.104	1.024	1.023	1.101
	Z	**NC**		0.990	0.993	0.987	0.995
	Y	**V**		0.978	0.824	1.494	1.436
N4-C17	X	**IL**	1.401	1.383	1.411	1.371	1.361
	Z	**IH**		1.427	1.425	1.434	1.500
	Y	**IH**		1.486	1.407	1.500	1.896

Bond	SMF along indicated Cartesian axis	Tendency*	Bond length [Å] at flux density [AFU]				
			0	0.1	1.0	10	100
N4-C20	X	**IH**	1.325	1.368	1.383	1.382	1.381
	Z	**V**		1.339	1.337	1.326	1.320
	Y	**IH**		1.480	1.476	1.365	1.772
C5-C6	X	**RH**	1.340	1.336	1.370	1.440	1.480
	Z	**V**		1.364	1.365	1.361	1.344
	Y	**IH**		1.246	1.432	1.457	1.582
C5-C24	X	**V**	1.458	1.472	1.473	1.350	1.375
	Z	**IH**		1.488	1.492	1.499	1.453
	Y	**RH**		1.478	1.597	1.656	1.671
C6-C7	X	**RL**	1.460	1.442	1.412	1.412	1.379
	Z	**V**		1.428	1.435	1.410	1.450
	Y	**V**		1.416	1.546	1.559	1.596
C6-H26	X	**V**	1.080	1.198	1.123	1.107	1.209
	Z	**IH**		1.098	1.100	1.171	1.113
	Y	**RH**		1.262	1.706	1.854	1.891
C7-C8	X	**V**	1.462	1.453	1.425	1.450	1.514
	Z	**IH**		1.490	1.495	1.493	1.500
	Y	**V**		1.568	1.398	1.429	1.671
C8-C9	X	**V**	1.326	1.307	1.398	1.388	1.396
	Z	**V**		1.366	1.365	1.359	1.395
	Y	**IH**		1.459	1.454	1.461	1.696
C8-H27	X	**V**	1.080	1.172	1.098	1.077	1.223
	Z	**RH**		1.084	1.086	1.094	1.124
	Y	**RH**		1.382	1.657	1.730	1.776
C9-C10	X	**RL**	1.456	1.445	1.428	1.424	1.441
	Z	**IH**		1.492	1.491	1.497	1.500
	Y	**IH**		1.562	1.532	1.547	1.802
C9-H28	X	**V**	1.080	1.129	1.094	1.091	1.150
	Z	**IH**		1.082	1.094	1.104	1.085
	Y	**IH**		1.459	1.499	1.408	1.911
C10-C11	X	**IH**	1.340	1.351	1.419	1.364	1.381
	Z	**V**		1.357	1.358	1.348	1.329
	Y	**IH**		1.418	1.418	1.383	1.587
C11-C12	X	**V**	1.460	1.407	1.397	1.428	1.417
	Z	**V**		1.426	1.430	1.433	1.429
	Y	**V**		1.452	1.463	1.341	1.778
C11-H29	X	**V**	1.080	1.160	1.141	1.076	1.179
	Z	**V**		1.104	1.105	1.097	1.103
	Y	**IH**		1.535	1.433	1.604	2.068
C12-C13	X	**RH**	1.337	1.380	1.380	1.382	1.480
	Z	**V**		1.435	1.430	1.426	1.430
	Y	**IH**		1.410	1.464	1.614	1.599
C13-C14	X	**NC**	1.450	1.400	1.395	1.425	1.431
	Z	**IL**		1.483	1.410	1.480	1.401
	Y	**V**		1.418	1.416	1.537	1.070
C13-H30	X	**V**	1.080	1.138	2.265	1.179	1.109
	Z	**V**		1.082	1.085	1.085	1.007
	Y	**V**		1.817	1.338	1.496	2.060

Bond	SMF along indicated Cartesian axis	Tendency*	Bond length [Å] at flux density [AFU]				
			0	0.1	1.0	10	100
C14-C15	X	**V**	1.337	1.342	1.408	1.403	1.401
	Z	**RH**		1.430	1.430	1.442	1.453
	Y	**IH**		1.406	1.392	1.507	1.620
C14-H31	X	**IH**	1.080	1.798	1.120	3.640	6.799
	Z	**IH**		1.083	1.086	1.127	1.079
	Y	**IH**		1.130	1.739	1.860	1.753
C15-C16	X	**V**	1.460	1.414	1.382	1.436	1.452
	Z	**V**		1.434	1.430	1.428	1.442
	Y	**IH**		1.378	1.454	1.495	1.633
C16-C17	X	**RH**	1.340	1.384	1.368	1.428	1.452
	Z	**IH**		1.355	1.358	1.362	1.329
	Y	**V**		1.316	1.428	1.518	1.497
C16-H32	X	**IH**	1.080	1.225	1.084	1.298	1.359
	Z	**NC**		1.104	1.105	1.098	1.103
	Y	**RH**		1.104	1.595	1.778	1.891
C17-C18	X	**V**	1.456	1.435	1.435	1.424	1.445
	Z	**V**		1.493	1.491	1.476	1.500
	Y	**RH**		1.504	1.508	1.560	1.671
C18-C19	X	**V**	1.337	1.357	1.320	1.418	1.417
	Z	**IH**		1.367	1.365	1.374	1.395
	Y	**IH**		1.387	1.527	1.482	1.696
C18-H33	X	**V**	1.080	1.198	1.085	1.200	1.232
	Z	**RH**		1.084	1.086	1.094	1.095
	Y	**RH**		1.276	1.547	1.568	1.776
C19-C20	X	**V**	1.452	1.448	1.453	1.386	1.384
	Z	**RH**		1.485	1.496	1.499	1.516
	Y	**V**		1.517	1.378	1.417	1.802
C19-H34	X	**V**	1.080	1.138	1.077	1.073	1.223
	Z	**RH**		1.083	1.086	1.094	1.971
	Y	**V**		1.521	1.494	1.407	1.911
C21-C22	X	**V**	1.340	1.364	1.389	1.365	1.344
	Z	**IH**		1.354	1.362	1.368	1.344
	Y	**IH**		1.401	1.324	1.656	1.770
C20-C21	X	**V**	1.460	1.418	1.402	1.451	1.472
	Z	**IL**		1.366	1.362	1.358	1.329
	Y	**V**		1.459	1.432	1.457	1.633
C21-H35	X	**V**	1.080	1.997	1.088	1.157	1.056
	Z	**V**		1.102	1.100	1.095	1.113
	Y	**IH**		1.567	1.465	1.614	2.068
C22-C23	X	**V**	1.458	1.441	1.428	1.520	1.584
	Z	**V**		1.485	1.492	1.475	1.453
	Y	**RH**		1.500	1.544	1.656	1.599
C23-C24	X	**V**	1.333	1.277	1.280	1.355	1.329
	Z	**RH**		1.357	1.362	1.368	1.397
	Y	**IH**		1.403	1.484	1.593	1.070
C23-H36	X	**V**	1.080	1.225	1.733	1.082	1.214
	Z	**V**		1.097	1.088	1.073	1.129
	Y	**IH**		1.528	1.445	1.623	2.060
C24-H25	X	**IH**	1.080	1.354	1.064	3.183	6.835
	Z	**NC**		1.084	1.088	1.083	1.096
	Y	**IH**		1.1591	1.689	1.839	1.753

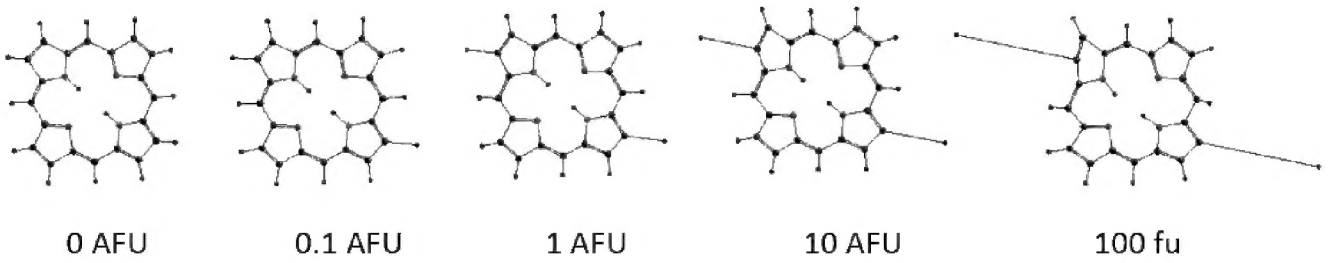

a

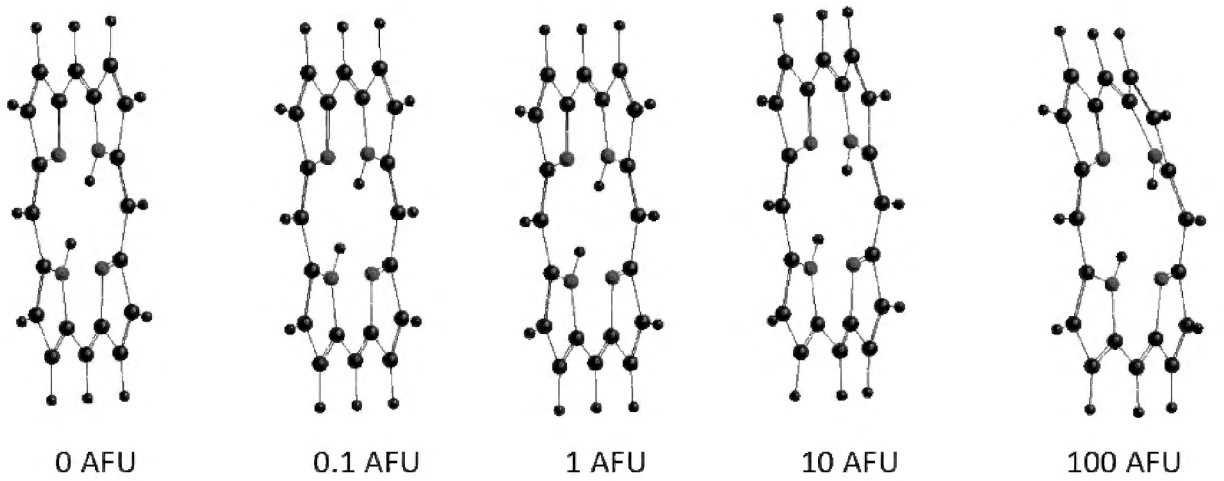

b

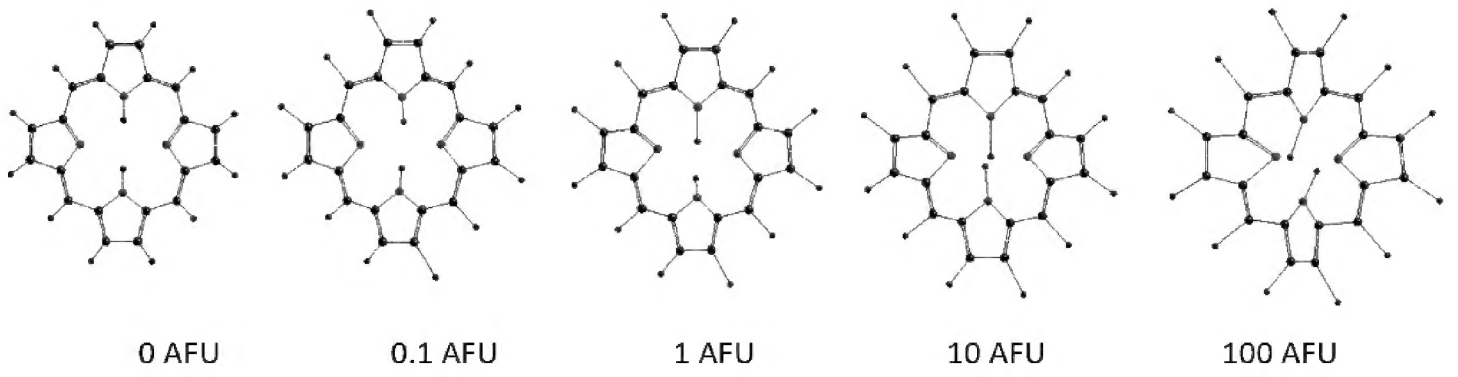

c

Figure 2. Deformation of the porphine molecule in SMF of flux density increasing from 0 to 100 AFU. The molecule was situated either in the x-y (a), y-z (b) or x-z (c) planes of the Cartesian system. SMF was applied along the x-axis.

Conclusions

The planar molecule of porphine deforms when placed in the static magnetic field. The deformation depends on the situating the molecule against the field. The deformation engages pyrrole rings holding the hydrogen atoms at the ring nitrogen atoms. The length of the C–H and N–H bonds is also an essential factor.

Data availability

All data underlying the results are available as part of the article and no additional source data are required.

References

Aylward N, Bofinger N (2005) Possible origin for porphin derivatives in prebiotic chemistry - a computational study. Origins of Life and Evolution of the Biosphere 35(4): 345–368. https://doi.org/10.1007/s11084-005-2044-x

Carpenter JE, Weinhold F (1988) Analysis of the geometry of the hydroxymethyl radical by the different hybrids for different spins natural bond orbital procedure. Journal of Molecular Structure (Teochem) 139: 41–62. https://doi.org/10.1016/0166-1280(88)80248-3

Caughey WS, Ibers JA (1977) Crystal and molecular structure of the free base porphyrin, protoporphyrin IX dimethyl ester. Journal of the American Chemical Society 99(20): 6639–6645. https://doi.org/10.1021/ja00462a027

Charistos ND, Muñoz-Castro A (2019) Double aromaticity of the B-40 fullerene: Induced magnetic field analysis of pi and sigma delocalization in the boron cavernous structure. Physical Chemistry Chemical Physics 21(36): 20232–20238. https://doi.org/10.1039/C9CP04223G

Ciesielski W, Girek T, Oszczęda Z, Soroka JA, Tomasik P (2021) Towards recognizing mechanisms of effects evoked in living organisms by static magnetic field. Numerically simulated effects of the static magnetic field upon simple inorganic molecules. F1000 Research 10: e611. https://doi.org/10.12688/f1000research.54436.1

Ciesielski W, Girek T, Oszczęda Z, Soroka JA, Tomasik P (2022a) Potential risk resulting from the influence of static magnetic field upon living organisms. Numerically simulated effects of the static magnetic field upon simple alkanols. BioRisk [in press].

Ciesielski W, Girek T, Kołoczek H, Oszczęda Z, Soroka JA, Tomasik P (2022b) Potential risk resulting from the influence of static magnetic field upon living organisms. Numerically simulated effects of the static magnetic field upon carbohydrates. BioRisk [in press].

Committee to Assess the Current Status and Future Direction of High Magnetic Field Science in the United States (2013) High Magnetic Field Science and Its Application in the United States; Current Status and Future Directions. Natl. Res. Council, National Acad., The National Academies Press, Washington, D.C.

Elder GH (1994) Haem synthesis and the porphyrias. In *Scientific Foundations of Biochemistry in Clinical Practice* (2nd Edn.). Williams DL, Marks V. (Eds), Imprint: Butterworth-Heinemann, Oxford, UK. https://doi.org/10.1016/B978-0-7506-0167-2.50029-7

Farberovich OV, Mazalova VL (2016) Ultrafast quantum spin-state switching in the Co-octaethylporphyrin molecular magnet with a terahertz pulsed magnetic field. Journal of Magnetism and Magnetic Materials 405: 169–173. https://doi.org/10.1016/j.jmmm.2015.12.038

Frisch MJ, Trucks GW, Schlegel HB, Frisch MJ, Trucks GW, Schlegel HB, Scuseria GE, Robb MA, Cheeseman JR, Scalmani G, Barone V, Mennucci B, Petersson GA (2016) Gaussian 09, Revision A.02, Gaussian, Inc., Wallingford.

Froimowitz M (1993) HyperChem: A software package for computational chemistry and molecular modelling. BioTechniques 14: 1010–1013.

Glendening ED, Reed AE, Carpenter JE (1987) Extension of Lewis structure concepts to open-shell and excited-state molecular species, NBO Version 3.1. Ph.D. thesis, University of Wisconsin, Madison, WI.

Hamza A-SHA, Shaher SA, Mohmoud A, Ghania SM (2002) Environmental pollution by magnetic field associated with power transmission lines. Energy Conversion and Management 43(17): 2442–2452. https://doi.org/10.1016/S0196-8904(01)00173-X

Kadish KM, Smith KM, Guilard R (Eds) (2000) Porphyrin Handbook, Academic Press, San Diego.

Magnet Science and Technology (2021) Magnet Science & Technology. https://nationalmaglab.org/magnet-development/magnet-science-technology [Retrieved 4th Jan. 2021]

Magnetism in real life (2021) http://www.scienceclarified.com/everyday/Real-Life-Physics-Vol-3-Biology-Vol-1/Magnetism-Real-life-applications.html [Retrieved 4th Jan. 2021]

Marchand N, Lienard P, Siehl H, Izato H (2014) Applications of molecular simulation software SCIGRESS in industry and university. Fujitsu Scientific and Technical Journal 50(3): 46–51.

Mazurkiewicz J, Tomasik P (2013) Effect of external electric field to porphine and selected metalloporphin systems. Journal of Alternative and Complementary Medicine (New York, N.Y.) 1: 13–21.

Ortiz de Montellano PR (2008) Hemes in Biology. Wiley Encyclopedia of Chemical Biology. John Wiley & Sons. https://doi.org/10.1002/9780470048672.wecb221

Rankovic V, Radulovic J (2009) Environmental pollution by magnetic field around power lines. International Journal of Qualitative Research 3(3): 1–6.